HYDROLOGICAL PROCESSES
Hydrol. Process. **28**, 868–881 (2014)
Published online 4 December 2012 in Wiley Online Library
(wileyonlinelibrary.com) DOI: 10.1002/hyp.9619

Sensitivity of model parameterizations for simulated latent heat flux at the snow surface for complex mountain sites

Michele L. Reba,[1]* Danny Marks,[2] Timothy E. Link,[3] John Pomeroy[4] and Adam Winstral[2]

[1] *Agricultural Research Service, National Sedimentation Laboratory, Jonesboro, AR, USA*
[2] *Agricultural Research Service, Northwest Watershed Research Centre, Boise, ID, USA*
[3] *University of Idaho, College of Natural Resources, Moscow, ID, USA*
[4] *Centre for Hydrology, University of Saskatchewan, Saskatoon, Saskatchewan, Canada*

Abstract:

The snowcover energy balance is typically dominated by net radiation and sensible and latent heat fluxes. Validation of the two latter components is rare and often difficult to undertake at complex mountain sites. Latent heat flux, the focus of this paper, is the primary coupling mechanism between the snow surface and the atmosphere. It accounts for the critical exchange of mass (sublimation or condensation), along with the associated snowcover energy loss or gain. Measured and modelled latent heat fluxes at a wind-exposed and wind-sheltered site were compared to evaluate variability in model parameters. A well-tested and well-validated snowcover energy balance model, *Snobal*, was selected for this comparison because of previously successful applications of the model at these sites and because of the adjustability of the parameters specific to latent heat transfer within the model. Simulated latent heat flux and snow water equivalent (SWE) were not sensitive to different formulations of the stability profile functions associated with heat transfer calculations. The model parameters of snow surface roughness length and active snow layer thickness were used to improve latent heat flux simulations while retaining accuracy in the simulation of the SWE at an exposed and sheltered study site. Optimal parameters for simulated latent heat flux and SWE were found at the exposed site with a shorter roughness length and thicker active layer, and at the sheltered site with a longer roughness length and thinner active layer. These findings were linked to physical characteristics of the study sites and will allow for adoption into other snow models that use similar parameters. Physical characteristics of wind exposure and cover could also be used to distribute critical parameters in a spatially distributed modelling domain and aid in parameter selection for application to other watersheds where detailed information is not available. Copyright © 2012 John Wiley & Sons, Ltd.

KEY WORDS latent heat flux; snow modelling; eddy covariance; roughness length; active layer thickness

Received 30 September 2011; Accepted 8 October 2012

INTRODUCTION

Much of western North America is subject to high spatiotemporal variability in snow accumulation, energetics and melt. This variability can be simulated with physically based snowcover energy balance models. Accurate modelling of the quantity and timing of melt, runoff and streamflow is of utmost importance as water supplies are scarce and over-allocated in many parts of this region. Most components of snowcover energy balance models are validated through direct measurements such as SWE, density, temperature and net radiation. However, validation data for turbulent fluxes are generally difficult to obtain. Eddy covariance (EC) is the most direct measurement of turbulent fluxes over snow and can be used to verify how turbulent fluxes vary seasonally and across the landscape. Understanding of the variability can be used to improve modelling of the turbulent fluxes. As shown by Marks *et al.* (2008), EC measurements can, after appropriate post-processing and correction, be used to validate the turbulent components of snowcover energy balance models.

Climate is expected to warm globally. In snow-dominated regions of western North America, the impacts of warming have been shown to impact snow deposition and melt (Cayan *et al.*, 2001; McCabe and Clark, 2005; Stewart *et al.*, 2005; Mote *et al.*, 2008). Warmer conditions and earlier melt dates may increase the number of mid-winter rain events and hence rain-on-snow events (Marks *et al.*, 1998; Marks *et al.*, 2001b). Trends generated from 45 years of meteorological data at an intermountain western watershed showed warmer temperatures, higher humidity and more winter rain (Nayak *et al.*, 2010). During rain-on-snow events, turbulent fluxes are the primary contributors to rapid changes in the snowcover energy balance that can cause rapid melt and result in extensive runoff and flooding (van Heeswijk *et al.*, 1996; Marks *et al.*, 2001b). These findings suggest a changing and unstable hydroclimatology for the western mountain regions. Under these conditions, historical relationships that are often used for calibration of models may be inappropriate. Models based on the physics of the process and that require little or no calibration will best suit the needs for future water resources management.

Eddy covariance is the most direct method available to measure fluxes of heat, water and carbon. Instrumentation has become more robust over the past few decades, which has allowed for increased use over snow in mountainous

*Correspondence to: Michele L. Reba, Agricultural Research Service, National Sedimentation Laboratory, Jonesboro, AR, USA.
E-mail: michele.reba@ars.usda.gov

basins (Harding and Pomeroy, 1996; Nakai *et al.*, 1999; Pomeroy *et al.*, 2003; Turnipseed *et al.*, 2003; Lee and Mahrt, 2004; Mahrt and Vickers, 2005; Molotch *et al.*, 2007; Marks *et al.*, 2008; Reba *et al.*, 2009). Reba *et al.* (2009) describe some of the challenges associated with using EC in complex terrain and conclude that the data collected at the described complex sites were of *high quality* (as defined by Rebmann *et al.*, 2005) after post-processing. Post-processing includes despiking (Vickers and Mahrt, 1997), wind data rotation (Kaimal and Finnigan, 1994), wind direction filtering, sonic temperature correction (Schotanus *et al.*, 1983), density correction (Webb *et al.*, 1980) and sensor heating correction (Burba *et al.*, 2008). Although EC sensors respond poorly during precipitation events, measurements made during between-storm conditions can be used to validate and improve physically based models and hence our understanding of processes that occur during extreme events. Additionally, energy balance closure discrepancies of 10–30% are reported and attributed to systematic bias in instrumentation, loss of low-frequency and/or high-frequency contributions and a mismatch of measurement scales of the energy balance components (Twine *et al.*, 2000; Wilson *et al.*, 2002). At extremely level sites with strong stability and poorly developed turbulence, there appear to be more substantial unmeasured atmospheric exchanges that EC corrections cannot compensate for (Helgason and Pomeroy, 2012b). Data quality can be improved by selecting only *high-quality* data that satisfy specific criteria of stationarity and well-developed turbulence (Rebmann *et al.*, 2005).

Turbulent transfer of sensible and latent heat is the most complicated form of energy exchange between the snow surface and the atmosphere to simulate (Marks and Dozier, 1992). Simulated values of latent heat flux and sublimation were shown to be hydrologically important (Marks *et al.*, 1998; Marks *et al.*, 1999; Marks *et al.*, 2002). Although simulated values are sometimes larger than expected and may over-estimate actual fluxes (Pomeroy *et al.*, 1998), only very limited validation data are available, and the data that are available are often from wind-sheltered sites such as that used by Marks *et al.* (2008). Latent heat flux measurements will be the focus of the analysis presented in this paper. During the snow season, latent heat flux from the snow surface is the primary source of the moisture flux to the atmosphere and hence is the critical exchange of mass (sublimation or condensation), along with the associated substantial energy loss or gain.

Two parameters that are particularly critical for simulation of the turbulent fluxes and are specified for most snow models are snow surface roughness (z_0) and the active layer thickness at the snow surface. In more complicated multilayer models (e.g. Anderson, 1976; Jordan, 1991; Flerchinger *et al.*, 1994), the use of an implicit solution to the energy balance equations allows the creation of many snow layers, which are continually adjusted throughout the simulation. In these models, the surface roughness is generally fixed, but the active layer thickness is adjusted as needed depending on the magnitude of thermal gradients at the time. Unfortunately, such models are computationally very demanding. Even with current computer technology, it is not possible to apply these models in a spatial context over raster grids of on the order of 10^6 to 10^7 cells and at hourly time steps for multiple years. Further, such models generally require that the structure of the snowcover be specified as an input parameter; this information is not commonly available and limits the use of such models. Because of problems with parameter identification and availability, such models have difficulty in simulating both the development and ablation of the snowcover without specialized observations to parameterize them.

In this experiment, we use the *Snobal* model, first described by Marks and Dozier (1992) (e.g. Marks *et al.*, 1998; Link and Marks, 1999b; Marks *et al.*, 2001b; Johnson and Marks, 2004; Marks *et al.*, 2008; Seyfried *et al.*, 2009a), which along with its spatial version *Isnobal* (Link and Marks, 1999a; Marks *et al.*, 2001b; Marks *et al.*, 2002; Winstral and Marks, 2002; Garen and Marks, 2005; Winstral *et al.*, 2009; Reba *et al.*, 2011b; Nayak *et al.*, 2012) has been applied to a multitude of sites across North America with varying snow and climate conditions. This model relaxes some of the detail of the more complicated models in favour of numerical efficiency. Using an explicit numerical approach represents the snowcover as a two-layer system, a fixed-thickness snow surface active layer and a lower layer representing the rest of the snowcover (see Marks *et al.*, 1999 for details of the model structure). Simulations are typically run over a full winter of a water year from the first of October to the end of July, and account for initiation, development and ablation of the snowcover.

Snow surface roughness (z_0) is generally specified as an initial condition before a snowcover energy balance model is applied. Roughness lengths are quasiphysical scaling parameters that are difficult to specify in a natural environment and are dependent on snow surface characteristics (Andreas, 1987). Snow surface roughness length for a specific model application is based on an understanding of both site and snowcover conditions and can be modified or updated during the simulation as changing conditions warrant. Values commonly range from 0.0001 to 0.01 m (Jordan, 1991; Marks and Dozier, 1992; Tarboton and Luce, 1996; Marks *et al.*, 2008; Andreadis *et al.*, 2009). Despite this range of values, little guidance exists on how snow surface roughness (z_0) should vary in time or space. Consequently, snow surface roughness (z_0) is often arbitrarily defined and assumed constant over the modelling domain and throughout the snow season.

All atmospheric interaction with the snowcover (shortwave and longwave radiation, sensible and latent heat flux) is assumed to be limited to a relatively thin layer near the snowcover surface. We define this layer as the *active layer* in *Snobal* and assume that atmospheric exchange processes are unable to penetrate directly to the snowcover below this layer. The exact thickness of the active layer has been debated (see Andreas, 1987; Nolin and Dozier, 1993) but is generally assumed to be no more than 0.25 m. The value seems to vary as a function of site and weather conditions,

with a thicker active layer during high winds and a thinner active layer during calm conditions (Marks *et al.*, 2008). In the research performed by Link and Marks (1999b), it was discovered that snow simulations that used a thinner layer were more accurate in the boreal forest. This was attributed to the very large temperature gradients between the atmosphere and the snow surface found in that region. In a thin or ephemeral snowcover, the entire system is 'active', whereas in a deep snowcover, the lower portion is insulated from the atmosphere by the active layer. The snowcover lower layer exchanges energy only by conduction, convection and advection with the active layer and the soil below.

In *Snobal*, the active layer thickness is an initial condition set by the user that is not changed during the simulation. As shown by Marks *et al.* (2008), it influences the magnitude of over-snow simulated turbulent fluxes. *Snobal* simulates exchanges between the mass-integrated temperature of the active layer snow volume and the atmosphere. If the active layer is too thick, thermal artefacts may occur in the simulation result. Specifically, early in the day, the active layer remains cold reducing turbulent fluxes even though insolation has warmed the snow surface. Late in the day, the active layer remains warm enhancing turbulent fluxes even though the snow surface is in shade and has cooled. Marks *et al.* (2008) showed that for a wind protected site, the magnitude of these artefacts depended, to a large extent, on the specified active layer thickness, and that they can be effectively eliminated by reducing the thickness to 0.10 m.

The overall objective of this study is to determine the specification of z_0 and active layer thickness that best reduces the difference between measured and simulated latent heat fluxes at relative extremes of exposure/shelter, while retaining the accuracy of simulated SWE. The overall objective was achieved by (1) determining if modification of the model stability profile functions is warranted on the basis of improvement to model performance and (2) determining generalized optimal active layer and roughness height parameters for the turbulent transfer calculations as a function of site characteristics and seasonality. This study takes advantage of post-processed EC data from two contrasting sites in complex terrain. These data were used to better quantify the range of turbulent flux conditions that can be expected in a mountain catchment, in order to more effectively specify initial conditions of z_0 and active layer thickness in *Snobal*. Ultimately, the findings will be used to determine how these parameters may be distributed across the landscape for application of the spatial model, *Isnobal*, or other models that use similar formulations for latent energy exchange.

METHODS

Site description

The data for this study were collected at the Reynolds Creek Experimental Watershed (RCEW) in southwestern Idaho, USA (Figure 1) (Marks *et al.*, 2001a). The study site, Reynolds Mountain East (RME), is a small catchment (0.4 km^2) in RCEW that ranges in elevation from 2028 to 2137 m.a.s.l. (Slaughter *et al.*, 2001). The catchment is characterized by large expanses of sagebrush and small wooded patches of fir and aspen that cover 34% of the catchment (Marks and Winstral, 2001). Conditions at RCEW are generally similar to much of the Great Basin with cool, wet winters and warm, dry summers, and a range of land cover characteristics ranging from isolated forest patches in sheltered areas to shrub, grass or rock at more exposed locations.

The two primary measurement study sites represent wind-exposed and wind-sheltered conditions in the RME catchment (Figure 2) and represent relative extremes of wind exposure and shelter where measurements of precipitation, meteorological conditions and EC parameters are feasible. These sites, referred to hereafter as *exposed* and *sheltered*, are indicative of the strong spatial heterogeneity in wind, snow deposition and meteorological parameters typical of this region. The vegetation at the exposed site is dominated by sagebrush, whereas the sheltered site is located in an aspen grove. The two sites studied have

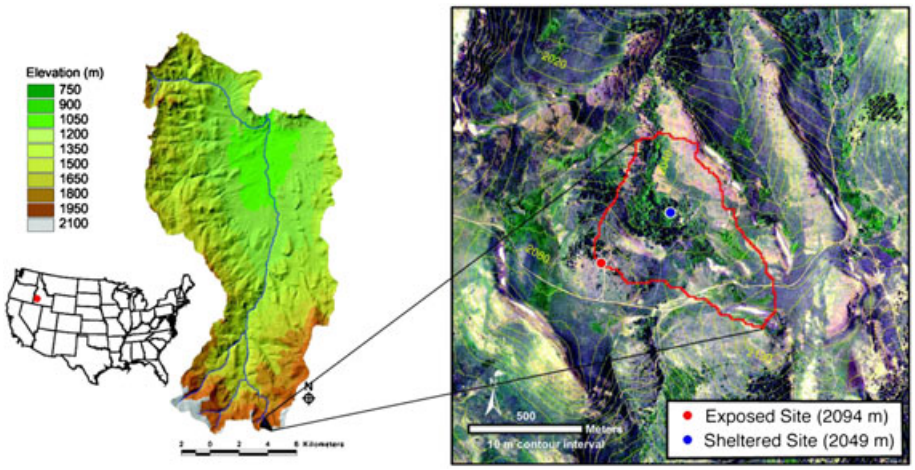

Figure 1. Reynolds Creek Experimental Watershed with inset of Reynolds Mountain East. The distribution of forest, shrub and bare ground are shown in the orthophoto

Figure 2. (a) An upwind view from the wind-exposed eddy covariance (EC) site, (b) the sheltered EC site, (c) an upwind view from the sheltered snow pillow site and (d) a downwind view from the sheltered snow pillow site. The sheltered EC site and sheltered snow pillow site are approximately 70 m apart

contrasting site conditions related to wind, vegetative cover and peak snow accumulation. Average water year wind-corrected precipitation is 556 mm at the exposed site and 996 mm at the sheltered site owing to preferential deposition and redistribution at the sheltered site (Hanson, 2001), 60–90% of which falls as snow (Nayak *et al.*, 2010). Although locations with both more extreme and intermediate exposure and shelter exist in RCEW, the sites were selected as effective end members given measurement and access limitations and to accomplish specific research objectives. Results from these sites should be useful for a wide range of wind speed conditions in cold regions mountain environments.

Meteorological and EC measurements from the exposed and sheltered sites in RME were used for this study. A snow pillow at the sheltered site was used to measure SWE. At the exposed site, the EC tower and the meteorological station are co-located, whereas at the sheltered site, the EC tower is located a short distance, approximately 70 m, from the meteorological station. As a result, the EC tower is slightly more sheltered by the aspen canopy than the meteorological station. Measurements of turbulent fluxes from the two EC towers were located at 5 and 4.5 m above the ground surface at the exposed and sheltered sites, respectively. The footprint source area model (Schmid, 1997) was used to estimate the land area near the tower that quantifies what the sensors on the tower are measuring, referred to as the source area. The results showed that the maximum source area location was 125 and 108 m from the EC towers at the exposed and sheltered sites, respectively. The maximum source areas are characterized by similar topographic and vegetation structure as the respective EC-tower sites.

Sensors at the two EC sites include an infrared gas analyser (LiCor 7500, LiCor Biosciences, www.licor.com), a three-dimensional sonic anemometer (CSAT-3, Campbell Scientific, www.campellsci.com) and a data logger (CR5000, Campbell Scientific, www.campellsci.com) programmed to collect data at 10 Hz. The snow pillow meteorological station has been operated since the early 1960s. Biweekly snow course measurements of depth and SWE have been made since 1961, continuous monitoring of SWE with a snow pillow since 1980 and continuous monitoring of snow depth since 1999 (Marks *et al.*, 2001a).

2006 snow season. Data from the 2006 snow season were used for this analysis because it included the most complete EC data record. Basin-wide snow season total precipitation was 1148 mm, 30% of which fell as rain. As discussed by Nayak *et al*. (2010, 2012), the 2006 snow season was warm and wet with an average air temperature of 0.5 °C above normal, high November–May temperatures and the highest storm dew point temperature of the five snow seasons analysed. Basin-wide 1 April SWE was 128% (681 mm) of average, and total seasonal stream discharge was about 145% (762 mm) of average.

The precipitation pattern in 2006 was similar to the largest snow season on record, 1984, with a large input of precipitation as snow. One noteworthy difference between 1984 and 2006, however, was that a substantial portion of the 2006 precipitation fell as rain (30% of total precipitation) early in the winter, whereas in 1984, there was less rain (21% of total precipitation) most of which occurred in the spring.

Measured data

Latent heat flux. Post-processing of raw 10 Hz EC data is discussed in detail in Reba *et al*. (2009), which includes statistical analysis for quality control (Vickers and Mahrt, 1997), determination of the appropriate averaging period (Vickers and Mahrt, 2003), sonic temperature correction (Schotanus *et al*., 1983), air density correction (Webb *et al*., 1980), coordinate rotation (Kaimal and Finnigan, 1994), corrections due to sensor heating (Burba *et al*., 2008) and removal of nonstationary data (Foken and Wichura, 1996). A two-dimensional rotation (Kaimal and Finnigan, 1994) was applied to the data and reduced vertical wind speeds to near zero during all periods of interest (Reba *et al*., 2009). Ten-minute fluxes were averaged over a longer time scale of 1 h to reduce sampling errors (Vickers and Mahrt, 1997) and for comparison purposes to the simulated model output. Latent heat flux is represented in this analysis as positive during deposition or condensation and negative during sublimation or evaporation. Gap filling of the EC-measured data was not used to focus on the EC measurements rather than filling procedures. Therefore, comparisons of EC-measured and EC-simulated latent heat flux presented in this manuscript use data only from periods when *high-quality* (Rebmann *et al*., 2005) EC measurements were collected.

The data recorded at the sheltered site showed higher maximum air temperatures, lower minimum temperatures, nearly 2 °C larger diurnal temperature range, and warmer mid-day temperatures than the exposed site. Generally, the sheltered site tended to be warmer during the day and colder at night than the exposed site. Aspen is deciduous, so in winter the leaves are off and the site is relatively open with more than 50% of the skyview unobstructed. The leafless deciduous trees reduce wind speed at the snow surface. During the day, even though the site is topographically shaded in early morning and late afternoon, the mid-day sun easily penetrates the canopy, warms the trunks and increases longwave radiation to the snow surface. Low wind velocities under the canopy also restrict turbulent transfer. Data from above and below the canopy indicate that over a 25-year period (water year 1984–2008) for the winter months of November through March, longwave radiation is 24 W m^{-2} larger below the canopy compared with that above the canopy. The exposed site is also in direct sun, but is not wind sheltered, and does not have additional longwave input from the bare aspen canopy.

At night, when turbulent mixing brings the snow surface temperature close to the air temperature at the exposed site, the air is very still amongst the aspen trunks at the sheltered site. Again, because of the relatively open aspen canopy, the snow at the sheltered site is more open to the sky and therefore is characterized by relatively large negative longwave radiation fluxes from the snow surface at night. The result is that there are very cold near-surface nighttime temperatures at the sheltered site compared with the exposed site.

Differences in air temperature and vapour pressure between the sites were small but were more pronounced later in the season. Snow season average EC-measured latent heat flux at the exposed site was two times the magnitude of EC-measured fluxes at the sheltered site. Differences in wind speed between the sites influenced the magnitude of measured fluxes more so than the small differences in measured air temperature and vapour pressure.

Snow water equivalent. In the study catchment, SWE was continuously measured only at the sheltered snow pillow site. The sheltered snow pillow site was co-located with the sheltered meteorological station, located approximately 70 m from the sheltered EC site. Measured snow density was calculated from measured SWE and snow depth at the snow pillow site. At the exposed site, where snow depth was continuously measured, the density from the snow pillow was used to estimate SWE. The density is relatively conservative, and the depth describes much of the variance between the sites. For this analysis, *Snobal*-simulated SWE values were compared with estimated SWE from the exposed site and measured SWE from the sheltered site.

Statistical metrics of model performance, including Nash–Sutcliffe model efficiency (ME) (Nash and Sutcliffe, 1970), root mean square difference (RMSD), mean bias difference (MBD) and relative mean bias difference (RMBD), were calculated for simulated SWE (see Green and Stephenson, 1986; Link and Marks, 1999b). ME is a test of how well the model captures the variability in the measured values. ME values nearest to 1.0 indicate that the model has perfectly accounted for the variation in measured values. RMSD and MBD indicate the difference and bias between measured and simulated values, and RMBD is the MBD divided by the mean of the measured values and indicates the relative bias.

Snobal model

Model description. The *Snobal* model used for this analysis is an extensively tested and well-validated two-layer snowcover energy and mass balance model

(Marks and Dozier, 1992). The model solves the snowcover energy and mass balance in one dimension and is available in both point-based and grid-based or spatial configuration (*Isnobal*) (Marks *et al.*, 1999). The model simulates both the development and ablation of the snowcover for the snow season. An explicit rather than an iterative energy balance solution and a relatively simple two-layer representation of the snowcover are employed to achieve computational efficiency.

The model has accurately simulated the accumulation, melt and mass over a range of basins varying from 1 to 2500 km^2 (Marks *et al.*, 1999; Winstral and Marks, 2002; Garen and Marks, 2005). The model is very robust and has been successfully applied and validated across a wide range of site and climate conditions (Marks *et al.*, 1998; Link and Marks, 1999b; Link and Marks, 1999a; Marks and Winstral, 2001; MacDonald *et al.*, 2009; DeBeer and Pomeroy, 2010). Although the primary validation for these efforts has been mass or SWE, detailed evaluations of wind fields and snow deposition (Marks *et al.*, 2002; Winstral and Marks, 2002; Winstral *et al.*, 2009), energy and mass exchange between the snow and soil (Seyfried and Grant, 2007; Seyfried *et al.*, 2009b) have been conducted. The direct validation of turbulent fluxes has been limited to the analysis of Marks *et al.* (2008), so this experiment provides a broader range of conditions, enabling the opportunity for additional validation using EC-measured data from multiple sites.

Turbulent energy transfer within *Snobal* is calculated with a method adapted from Brutsaert (1982) by Marks and Dozier (1992) and described in detail in Reba *et al.* (2011a). The method uses a system of nonlinear equations to simultaneously solve for the Obukhov stability length L (m), friction velocity u^* ($m\,s^{-1}$), the sensible heat flux H ($W\,m^{-2}$) and the mass flux by sublimation from or condensation to the snow surface E ($W\,m^{-2}$). Latent heat flux L_vE ($W\,m^{-2}$) is calculated by multiplying L, latent heat of vaporization or sublimation ($J\,kg^{-1}$) by the mass flux. L varies with temperature and the state of the water (liquid or solid). Stability profile functions necessary for the iterative solution used in the model for stable conditions were adapted from Webb (1970) and for unstable conditions from Paulson (1970).

Snobal was selected for both its general and specific characteristics. The model code was easily accessible and modifiable, and the two input parameters that strongly affect simulated turbulent flux – snow surface roughness and active layer thickness – can be set by the user. The snow surface roughness is a quasiphysical scaling parameter used in the model. The zero plane displacement is calculated as a function of z_0 according to Paeschke (1937). The active layer is the upper layer that is in contact with the atmosphere and with the lower snow layer. Typically, the active layer is set at 0.25 m. Previous work indicated that the model is sensitive to active layer thickness in a low-wind, sheltered environment (see Marks *et al.*, 2008), but the sensitivity to this parameter in a wind-exposed environment has not been explicitly tested. Information across a range of turbulent conditions is required to determine how optimal values of snow surface roughness (z_0) and active layer thickness vary with site characteristics such as wind exposure and vegetation cover. This information will better inform the distribution of values for these parameters within the modelling domain used for spatial simulations.

Model application. Simulated and measured latent heat fluxes and SWE were analysed for the 2006 snow season. The overall goal was to improve or retain simulated SWE accuracy while determining the model parameters associated with accurately simulating latent heat flux. It is important to examine SWE and latent heat flux separately in evaluating snow hydrology model performance. The accuracy of simulated SWE values integrates components of the entire energy balance calculation without evaluating each component individually. In unsaturated conditions, there is potential for errors in components of the energy balance to sometimes compensate for each other without substantially degrading the results of snowmelt calculations, but in the more rare, and hydrologically important, saturated conditions, these energy balance errors accumulate to large errors in melt rate and hence spring SWE.

Eddy covariance-measured values from snowcover initiation (1 December 2005) to meltout were analysed. The snowcover was established earlier and remained later in the season at the sheltered site compared with that at the exposed site. The snow season averages and diurnal trends presented in this paper include data from snowcover initiation through meltout at the exposed site (3 May 2006).

An extensive body of knowledge has been devoted to improving formulations for the stability profile functions used in the calculation of turbulent fluxes (e.g. Brutsaert, 2005). Both stable and unstable conditions occurred during the study period, and to test the stability functions, combinations of stability functions were tested. For stable conditions, the formulation of Webb (1970) was tested against Cheng and Brutsaert (2005) and Brutsaert (1982). For unstable conditions, the formulation of Paulson (1970) was tested against Kader and Yaglom (1990). All combinations of unstable and stable configurations described were tested. Yasuda (1988) presents both stable and unstable configurations, which were tested against the previously mentioned combinations.

The snow surface roughness length used in *Snobal* is typically determined through user experience and existing literature. To determine the sensitivity of snow simulations to the magnitude of the roughness, length values of 0.0001, 0.0005, 0.001 and 0.003 m were used. Because simulations with a snow surface roughness length of 0.005 m became numerically unstable, roughness length greater than 0.003 m was not used. Numerical instability in *Snobal* occurs when a combination of decreased measurement height (deep snow), a large temperature gradient and low wind speeds results in difficulty in reaching an adequate solution. This typically occurs at very low wind speeds when fluxes are small – conditions

typical at the sheltered site. Generally, roughness length values greater than 0.005 m will produce a stable solution at the exposed site.

The default active layer thickness used in *Snobal* is 0.25 m. Findings from Marks *et al.* (2008) showed that a reduction to 0.15 m better aligned the diurnal timing of the measured and simulated turbulent fluxes at a below canopy conifer site in Colorado. To determine the optimal active layer thickness at these two sites, 0.25, 0.15, 0.10, 0.05 and 0.01 m were tested.

RESULTS AND DISCUSSION

Stability profile function modifications

Alteration of the existing stability profile functions within the model with alternate formulations produced almost no difference in model results. At the exposed site, the range of differences in latent heat fluxes produced by using recent formulations for the stability functions (Brutsaert, 1982; Yasuda, 1988; Kader and Yaglom, 1990; Cheng and Brutsaert, 2005) was only 1.4 W m^{-2} or 0.045 mm day^{-1} and only 8 mm of sublimation over the entire 2006 snow season. At the sheltered site, these differences were 0.1 W m^{-2} or 0.0032 mm day^{-1}, totaling only 0.6 mm of sublimation over the season. Evaluation of simulated and measured SWE resulted in a slightly reduced Nash–Sutcliffe ME (0.99 to 0.98) at the sheltered site and slightly increased ME at the exposed site (0.87 to 0.88). The difference in the results using the different functions is less than the accuracy with which latent heat flux can be measured and suggests that the model is not sensitive to different configurations of stability profile functions at the two study sites.

Although updating the stability profile functions in the model would keep the existing model current with recent theoretical developments, it does not appear to be required to improve model performance at the two sites and was therefore not justified. Furthermore, uncertainties in the applicability of recent theoretical developments to field calculations of turbulent fluxes may not warrant the modification (Helgason and Pomeroy, 2012b; Helgason and Pomeroy, 2012a).

Measured and simulated latent heat flux and snow water equivalent

Latent heat flux. The mean differences over the snow season between the simulated and EC-measured latent heat flux with different values of snow surface roughness length (z_0) are shown in Table I. Roughness length influenced the magnitude of the differences at the exposed site but had little influence at the sheltered site. Differences ranged from +7 to −7 W m^{-2} but were minimized at the exposed site using z_0 values of 0.0005 or 0.001 m. Differences at the sheltered site for latent heat flux appear to be unaffected by changing the value of z_0 and were only slightly improved (6 W m^{-2} difference compared with 7 W m^{-2}) by using a snow surface roughness length of 0.003 m.

Table I. Mean difference between simulated and measured latent heat flux at the exposed and sheltered sites for various roughness lengths during the snow season of 2006

z_0	0.0001 m	0.0005 m	0.001 m	0.003 m
Exposed site (W m^{-2})	7	2	−1	−7
Sheltered site (W m^{-2})	7	7	7	6

There was extensive variability in the measured values of z_0. At the exposed site, the measured values of z_0 were more consistent, with nearly all values less than 0.1 m, whereas at the sheltered site, approximately 12.5% of the values were larger than 0.1 m. The exposed site mean z_0 was 0.0055 m, and the median value was 0.00007 m, but after removing the largest 1% of the values, the mean was reduced to 0.002 m – a value identical to exposed sites on the Canadian Prairies when no snow saltation was occurring (Pomeroy and Gray, 1995). The sheltered site mean z_0 was 0.06 m, and the median value was 0.002 m, but after removing the largest 1% of the values, the mean was reduced to 0.04 m. These values follow the general trend of smaller values at sites with smoother surfaces like the exposed site and larger values at sites with more roughness elements like the sheltered site.

Varying the active layer thickness through different values from the default of 0.25 to 0.01 m influenced the magnitude of the mean differences between simulated and EC-measured latent heat flux by less than 1 W m^{-2} at both sites for all selected roughness lengths. However, the diurnal shape and timing of peak latent heat flux were influenced by the active layer thickness.

To evaluate the timing of the simulated and EC-measured latent heat flux over a snow season diurnal cycle, the average for each hour of the day for the snow season was calculated for both fluxes. Figure 3 shows the combined influence of the snow surface roughness length and active layer thickness used for the diurnal simulations. Roughness lengths of 0.0005 and 0.001 m minimized the difference between measured and simulated latent heat flux values at the exposed site. Peak simulated latent heat flux lagged the EC-measured peak by 3 h with an active layer thickness of 0.25 m. The lag was roughly 2 h with active layer thicknesses of 0.15 and 0.10 m, and 1 h with an active layer thickness of 0.05 m. A reduction to 0.01 m aligned the timing of the peak latent heat flux with the measured peak.

A thinner active layer represents less mass and therefore has less thermal inertia. A thinner active layer numerically responds more quickly to changes in temperature and turbulence between the atmosphere and the snow surface. This is particularly important at the sheltered site where wind speeds are low, and which can hence result in large thermal gradients near the snow surface. The thinner active layer better represents the actual part of the snow cover that is interacting with the atmosphere. However, at exposed sites, the differences are not as important because of more turbulence, which results in smaller near-surface thermal gradients. At the sheltered site, the differences are more pronounced because of low wind speeds and less

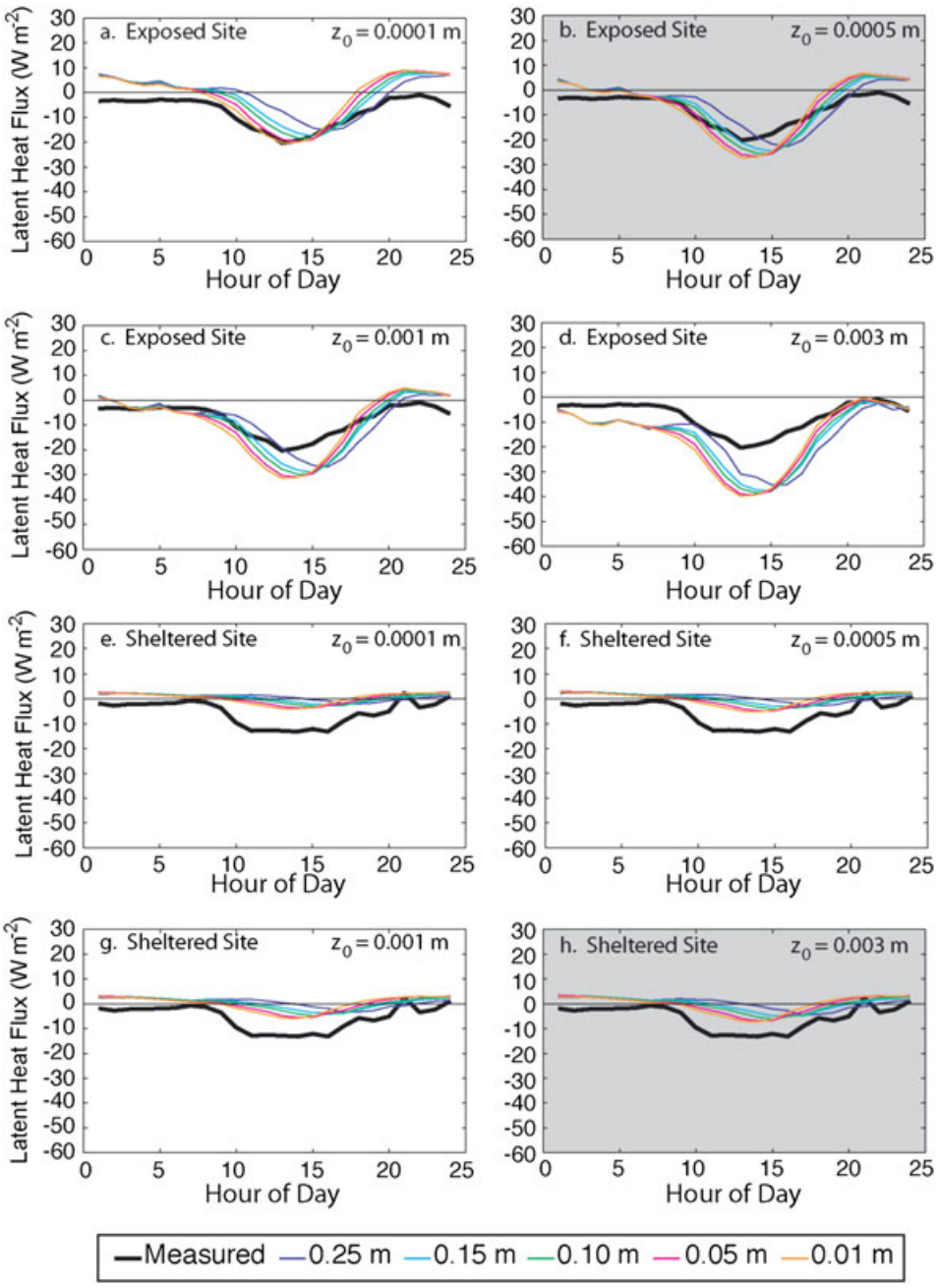

Figure 3. Simulated and measured latent heat flux (W m^{-2}) with various active layer thicknesses at the exposed site for snow surface roughness lengths of (a) 0.0001 m, (b) 0.0005 m, (c) 0.001 m and (d) 0.003 m, and at the sheltered site for snow surface roughness lengths of (e) 0.0001 m, (f) 0.0005 m, (g) 0.001 m and (h) 0.003 m for the 2006 snow season. The roughness length that presents the best fit is shaded for both sites

turbulence, and hence, the simulations are improved with thinner active layers.

A reduced active layer thickness forces the model to assign an average temperature to a thinner layer with less mass and thermal inertia so that it responds more quickly to changes in forcing even with low turbulence. This is particularly important in the afternoon hours after the site is shaded when the surface of the snow has cooled, but the temperature at 0.15–0.20 m depth is still relatively warm. At the exposed site, differences between EC-measured and EC-simulated values over the entire day were minimized using an active layer thickness of 0.15 m and a roughness length of 0.0005 m. Active layer thicknesses of 0.01 and 0.05 m caused simulated latent heat to accurately track the mid-day maximum flux but returned to near zero values too quickly in the afternoon. Therefore, the EC-measured diurnal cycle of the latent heat flux at the exposed site is best matched with a roughness length of 0.0005 m and an active layer thickness of 0.15 m.

At the sheltered site, mean EC-measured values were 5–8 W m^{-2} greater than simulated values. The difference of 5–8 W m^{-2} is approximately 40–60% of the measured flux for all combinations of snow surface roughness and active layer thickness. A 0.05 m active layer thickness produces a slightly better fit than the 0.25, 0.15 and 0.10 m thicknesses with the 0.003 m surface roughness length when compared

with the EC-measured diurnal flux pattern (Figure 3). A 0.10 and 0.15 m thickness yields a better fit than 0.25 m for a 0.003 m surface roughness length. It is possible that a larger roughness length would further improve the simulation. However, very low wind speeds at the sheltered site, coupled with the use of a larger roughness length, caused numerical instabilities in the simulation. Differences between all combinations of surface roughness and active layer thickness did not exceed 1–2 W m^{-2} because of low wind speeds at the sheltered site.

Snow water equivalent. As the overarching goal of modelling seasonal snowcover is to accurately track accumulation and ablation dynamics, the optimum input parameters for turbulent flux must improve or at least not degrade simulation accuracy for SWE. In this study, we assume that EC-measured latent heat flux is the most defensible measurement of the snow surface latent heat flux. If the difference between simulated and EC-measured latent heat flux is reduced, that should lead to an unchanged or improved simulation of snow ablation. The point model, *Snobal*, was applied to the exposed and snow pillow sites for the 2006 snow season using a range of roughness lengths from 0.0001 to 0.003 m. From this analysis, the optimal surface roughness for each site was selected and used to test a range of active layer thicknesses at each site in relation to the simulation of SWE.

Simulations of accumulation and melt at the exposed and snow pillow sites are presented for the 2006 snow season (Figure 4). A range of roughness lengths and a fixed active layer thickness of 0.25 m were used for the simulations presented in Figure 4 to better illustrate the influence roughness length had on SWE at both sites. Generally, simulations at the exposed site showed a wider range of response to slight modifications to snow surface roughness length than at the sheltered snow pillow site.

The mass traces shown in Figures 4a and 5a for the exposed site are not based on a measurement but on an estimate of SWE, using measured snow depth at the exposed site, and calculated density from the measured depth and SWE at the sheltered snow pillow site. The errors associated with this estimate are particularly exaggerated at shallow depths, which occur in November and early December. In addition, the depth sensor at the exposed site is somewhat unreliable during the early season because of exposed vegetation, and hence, the relationship between density at the snow pillow and density at the exposed site is poor. In general, once the vegetation is covered and snowcover is established, these issues diminish and the data become more reliable. The analysis presented here rejects the early season SWE data at the exposed site due to these data quality concerns.

At the exposed site, mean 2006 snow season SWE was 288 mm, and peak SWE (374 mm) occurred on 12 April. Roughness lengths of 0.0005 and 0.001 m tracked the mass better than both smaller and larger roughness length values as shown by the comparison statistics (Table II). Roughness lengths of 0.0005 and 0.001 m showed just over 30 mm of difference between measured and simulated SWE, with little or no bias, and yielded essentially the same ME. However, a roughness length of 0.0005 m yielded slightly smaller bias compared with using a roughness length of 0.001 m. Roughness lengths smaller than 0.0005 m or larger than 0.001 m yielded much smaller ME values and a larger bias.

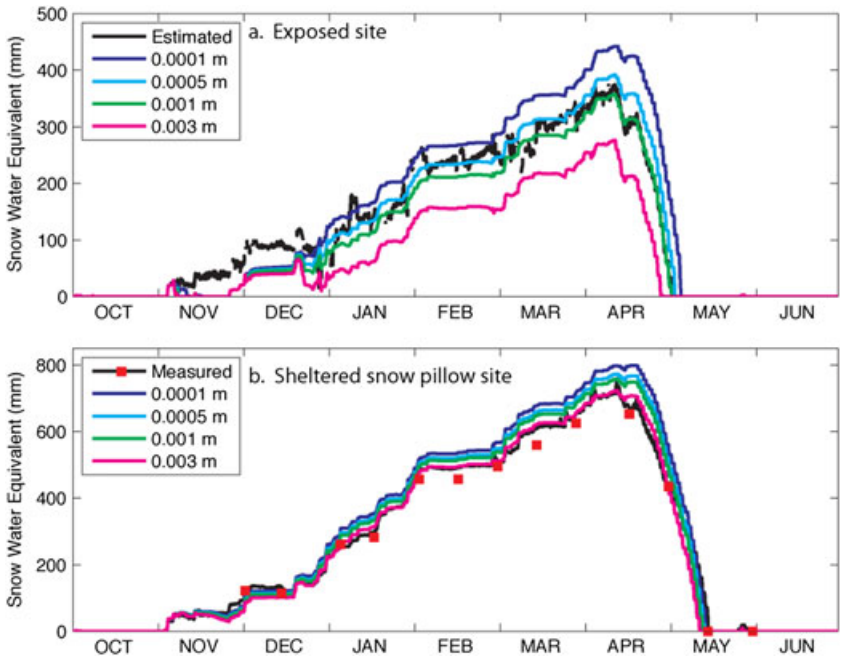

Figure 4. (a) Estimated and simulated SWE (using various roughness lengths) at the exposed site. Peak SWE during the 2006 snow season at this site was 374 mm. Problems with the depth sensor at the exposed site are shown early in the season. (b) Measured (both with the automated snow pillow: black line and snow survey: red points) and simulated SWE at the snow pillow site during the 2006 snow season. Peak SWE at this site was 758 mm. Note that the scales on (a) and (b) are different. Simulations use the default active layer thickness of 0.25 m

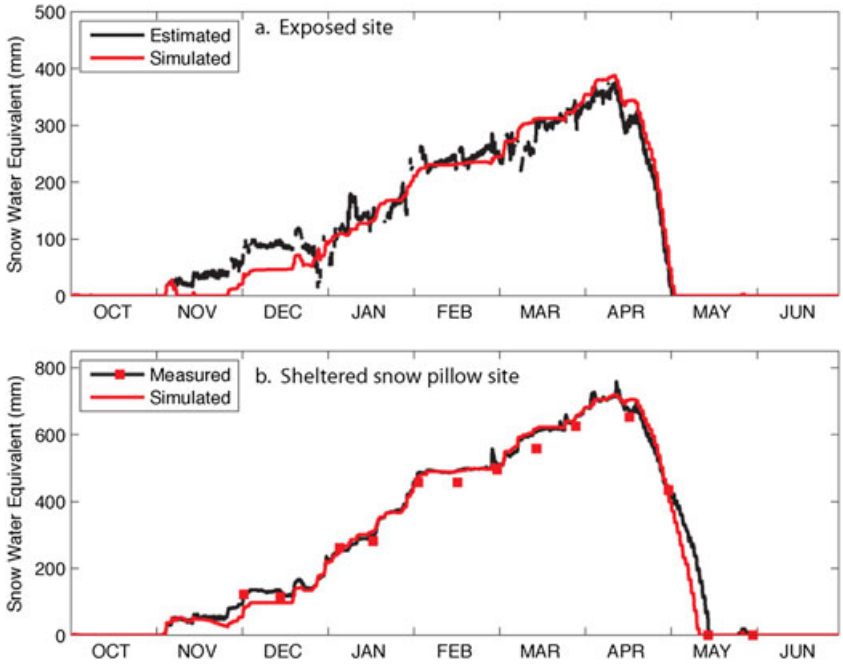

Figure 5. (a) Estimated and simulated SWE with optimal 0.0005–0.001 m snow surface roughness and 0.15 m active layer thickness for exposed site, (b) measured (both with the automated snow pillow: black line and snow survey: red points) and simulated SWE with optimal 0.003 m snow surface roughness and 0.15 m active layer thickness for snow pillow site. Note that the scales on (a) and (b) are different

As discussed, roughness length values of 0.0005 m and 0.001 m yielded the highest ME for the exposed site, and the smallest difference and bias values. The comparison statistics, however, do not illustrate the seasonality of the roughness length. Early in the snow season, a roughness length of 0.0005 m resulted in simulations that best track the estimated SWE measurement best. Prior to peak SWE and to the end of the season, a roughness length of 0.001 m tracks the estimated SWE measurement best (Figure 4a). The difference may be a reduction in instances of extreme stability in spring compared with that in mid-winter.

At the snow pillow site, the 2006 snow season mean SWE was 651 mm, and peak SWE (758 mm) occurred on 13 April 2006. As shown in Figure 4b, the SWE was accurately simulated using different roughness lengths at the snow pillow site, but the longer roughness length (0.003 m) best matches measured SWE. ME values were highest for a roughness length of 0.003 m (ME = 0.99) with an RMSD of 17 mm and essentially no bias. Shorter roughness lengths tested at the snow pillow site generated high ME values (>0.89) (Table III) but showed more difference and bias than the 0.003 m roughness length.

These results are also reflected in the analysis of the meltout date (Table IV). Meltout date and time are easily measured and are considered a good indication of model performance. However, because the model is forced with data (precipitation and meteorological parameters) that

Table II. Comparison statistics for simulated snow water equivalent (SWE) and estimated SWE derived from measured depth and estimated density from the exposed site (mean season SWE 288 mm, peak SWE 374 mm) using *Snobal* for the 2006 snow season with various roughness lengths and the default active layer thickness of 0.25 m

z_0	0.0001 m	0.0005 m	0.001 m	0.003 m
ME	0.51	0.86	0.87	0.21
RMSD (mm)	60	32	31	76
MBD (mm)	33	3	-18	-65
RMBD (%)	15	1	-8	-30

ME, model efficiency;RMSD, root mean square difference; MBD, mean bias difference; RMBD, relative mean bias difference.

Table III. Comparison statistics for simulated and snow pillow measured snow water equivalent (SWE) from the snow pillow site (mean season SWE 651 mm, peak SWE 758 mm) using *Snobal* for the 2006 snow season with various roughness lengths and an active layer thickness of 0.25 m

z_0	0.0001 m	0.0005 m	0.001 m	0.003 m
ME	0.89	0.94	0.97	0.99
RMSD (mm)	64	46	36	17
MBD (mm)	53	36	26	2
RMBD (%)	12	8	6	0

ME, model efficiency;RMSD, root mean square difference; MBD, mean bias difference; RMBD, relative mean bias difference.

Table IV. Difference between simulated and measured meltout (days) as a function of roughness length with the default active layer thickness of 0.25 m

z_0	0.0001 m	0.0005 m	0.001 m	0.003 m
Exposed site	−3	−1	0	+3
Snow pillow site	+1	+2	+3	+4

are generalized over a grid cell of at least 10–30 m, in general, simulating the timing of meltout within a day or two at a shallow snow site and within a few days at a deep snow site is considered very good. At the exposed site, the simulated meltout day matched the measured meltout using a roughness length of 0.001 m and was 1 day later with 0.0005 m. With shorter or longer roughness lengths, the simulated meltout date was 3 days later or earlier. At the sheltered site, simulated meltout dates were all earlier than the measured meltout date (Table IV). This is due in part to a snow pillow measured decrease in the melt rate in late April that was not simulated by the model (see Figure 5b) and by the fact that the snow pillow tends to meltout later than the surrounding area because it eliminates vapour and heat exchange with the soil. This causes the snow on the pillow to be colder than snow that is in contact with the soil (see Johnson and Marks, 2004). The 0.003 m roughness length caused simulated meltout to occur 4 days early. This is not unexpected as this is a deep snow site, and meltout on the snow pillow tends to be later than the surrounding area.

Variation of the active layer thickness had less influence on SWE model performance at the two sites. With the aforementioned assessment of the effect of different values for surface roughness on model performance, a snow surface roughness of 0.0005 m during snowcover development, and 0.001 m during ablation, was determined for the exposed site, whereas a snow surface roughness of 0.003 m was determined for the snow pillow site (Figure 5). At the exposed site, a reduction to a 0.15 m active layer thickness improved ME to 0.89 and reduced RMSD to 28 mm, MBD to −2 mm and RMBD to 1% (Table V). At the snow pillow site, changes in active layer thickness had no effect on the comparison statistics of measured and simulated mass, and the latent heat flux differences with different active layer thickness were very slight. Therefore, an active layer thickness of 0.15 m is recommended for both sites because of improved latent heat flux timing.

For both sites, the *Snobal* SWE simulation results match and track measured values, and the EC-measured and simulated turbulent fluxes agree; however, it is always possible that apparent validation of one parameter can be due to multiple compensating errors. There is evidence that this possibility is low, given the wealth of independent forcing and validation data at RME, and the reliable simulation of latent heat flux and SWE regime, including snow cover initiation and meltout at multiple sites, over a wide variety of snow and climate conditions. In addition, Reba *et al*. (2011b) ran the spatial version of the model for 25 snow seasons (1984–2008) in the same basin, and Garen and Marks (2005) successfully ran the model over the 2500 km^2 Boise River basin for multiple years with good results across a wide variety of wet, dry, warm and cold climate conditions. Although there may be differences or errors between measured and simulated parameters that could cancel each other, these are unlikely to be large and would not alter the results or conclusions of this study.

Table V. Comparison statistics for snow water equivalent from the exposed and snow pillow sites using *Snobal* for the 2006 snow season with an active layer thickness of 0.15 m and optimal roughness lengths derived from site characteristics

	ME	RMSD (mm)	MBD (mm)	RMBD (%)
Exposed site	0.89	28	−2	−1
Snow pillow site	0.99	17	−2	0

ME, model efficiency;RMSD, root mean square difference; MBD, mean bias difference; RMBD, relative mean bias difference.

SUMMARY

At the exposed site, simulations of mean latent heat flux best matched EC-measured values using roughness lengths of 0.0005 and 0.001 m during melt with differences of approximately 2 and $-1\,W\,m^{-2}$, respectively. In agreement with previous work by Marks *et al*. (2008), a reduced active layer minimized differences and best aligned the timing of the diurnal trend between simulated and EC-measured latent heat flux. The simulation was not sensitive to additional reductions in the active layer thickness beyond 0.15 m. Figure 5a shows exposed site mass simulation for the 2006 snow season using the optimal snow surface roughness (0.0005 m during snowcover development and 0.001 m during ablation) and 0.15 m active layer thickness.

At the sheltered site, the snow season differences in measured and simulated latent heat flux were essentially the same for the roughness lengths and active layer thicknesses tested and ranged from 7 to $6\,W\,m^{-2}$. The diurnal trend with a roughness length of 0.003 m yielded the smallest difference between simulated and measured latent heat flux values with active layer thicknesses of 0.05 and 0.01 m. At the snow pillow site, ME values for SWE were nearly perfect for a roughness length of 0.003 m, and these values were unaffected by reducing active layer thickness. Using optimal values of 0.15 m for the active layer thickness and 0.003 m for snow surface roughness resulted in ME of 0.99, RMSD of 14 mm, MBD of 2 mm and RMBD of 0%. This suggests that either the other components of the energy balance may be compensating for deficiencies in the latent heat flux simulations at the sheltered site or the EC measurements at the sheltered site may be unreliable. It is likely that some of both are occurring. Figure 5b shows mass simulation for the 2006 snow season at the snow pillow site using the optimal 0.003 m surface roughness and 0.15 m active layer thickness. Table V shows the final comparison statistics for the optimal model configurations at both sites.

Although EC is the most reliable method available to effectively measure turbulent fluxes, EC data collection is difficult, and processing and analysis of the data are very time consuming. Although in this paper we are treating EC results as a ‘measurement’, it is in reality a ‘model’ of

fluxes based on a theory of turbulence and on very high-frequency sampling of temperature, humidity and wind. The EC 'model' is least reliable in low wind speed environments, such as the sheltered site, where turbulent structure is less developed, but can also be unreliable in smooth snow environments where fully turbulent conditions may not always exist. The fact that EC-measured and *Snobal*-modelled fluxes agree as well as they do and that the simulated and measured SWE matches at both the sheltered and exposed sites supports the conclusion that the *Snobal* simulations are robust and reliable.

CONCLUSIONS

This study took advantage of thoroughly post-processed EC data from two contrasting sites in complex terrain to determine parameters used in an existing snowcover mass and energy balance model, *Snobal*. The profile functions used in *Snobal* were evaluated to determine if updating was necessary or advantageous. The model results under the conditions that occurred during the 2006 snow season were not sensitive to these functions but may be for other locations or ranges of conditions.

The exposed site is an exemplar of open, windy snow sites, whereas the sheltered site is an exemplar of sheltered deciduous forest sites. The sheltered site is very important to local hydrology as it receives as much as 25–30% of areal snow deposition and provides meltwater late into the spring period. These two sites represent the range of conditions under which the experiment presented in this paper was possible and represent a reasonable range of conditions that should be considered when modelling turbulent transfer to snowy environments.

This research showed that site conditions and wind exposure influence the value of snow surface roughness used for modelling. The snow surface roughness lengths determined for the two study sites are also linked to site-specific conditions. Larger roughness elements below the forest canopy at the sheltered site required a larger roughness length to account for low wind conditions. The smoother surface at the exposed site required a smaller roughness length. A shift in the optimal snow surface roughness at the exposed site from winter to spring may be due to the effect of greater stability in mid-winter than spring, whereas light winds at the sheltered site indicate that a single value is adequate. As the sagebrush at the exposed site is progressively exposed during spring, the snow surface roughness length should also increase. This study has shown that at the exposed site, a slightly longer snow surface roughness length yielded a more accurate simulation of SWE later in the season.

Analysis of measured and simulated latent heat flux and SWE allowed for the determination of the optimal input parameters of roughness length and active layer thickness while retaining accuracy in the seasonal snow accumulation and melt. Direct measurements of latent heat flux over snow in complex terrain are expensive and require extensive post-processing. Where available, they can be used to improve snowcover modelling. Findings of optimal values of roughness length and active layer thickness for modelling snow accumulation and ablation, and latent heat flux were related to site characteristics.

This study has provided information on how we may update and improve parameterization of snow surface roughness (z_0) and active layer thickness within the *Snobal* model. It is possible that the findings from this study could be incorporated into snow models that simulate turbulence in similar fashions or utilize similar parameters to characterize site conditions. More specifically, these findings can be incorporated into parameterizing the spatially distributed version of *Snobal* (*Isnobal*) using a combination of wind exposure and canopy structure characteristics (e.g. Winstral and Marks, 2002).

This research has extended our understanding of latent heat flux as a component of simulated snow cover energetics in complex mountainous terrain. It illustrates the importance of wind exposure and site conditions in mountain basins. It further illustrates the concept presented by Marks *et al.* (2008) that EC-measured fluxes can be used to validate and improve snow hydrology models.

ACKNOWLEDGEMENTS

The research and analysis presented in this paper were funded by the USDA Agricultural Research Service with support from the NOAA GEWEX Americas Prediction Project (GAPP) (project GC03-404). The Idaho EPSCoR and University of Idaho Graduate Fellowship Programmes provided additional support to the lead author. Additional support was provided by NSF-CBET Award No. 0854553, NSERC and the Canada Research Chairs programme.

REFERENCES

Anderson EA. 1976. A point energy and mass balance model of a snow cover. In *NWS Technical Report*. National Oceanic and Atmospheric Administration: Washington, DC; 150.

Andreadis K, Storck P, Lettenmaier D. 2009. Modeling snow accumulation and ablation processes in forested environments. *Water Resouces Research* **45**: W05429.

Andreas EL. 1987. A theory for the scalar roughness and the scalar transfer coefficients over snow and sea ice. *Boundary-Layer Meteorology* **38**: 159–184.

Brutsaert W. 1982. *Evaporation into the Atmosphere*. D. Reidel: Dordrecht; 299.

Brutsaert W. 2005. *Hydrology an Introduction*. Cambridge University Press: Cambridge, UK; 605.

Burba GG, McDermitt D, Grelle A, Anderson DJ, Xu L. 2008. Addressing the influence of instrument surface heat exchange on the measurements of CO2 flux from open-path gas analyzers. *Global Change Biology* **14**: 1854–1876.

Cayan D, Kammerdiener S, Dettinger M, Caprio J, Peterson D. 2001. Changes in the onset of spring in the Western United States. *Bulletin of the American Meteorological Society* **82**: 399–415.

Cheng Y, Brutsaert W. 2005. Flux–profile relationships for wind speed and temperature in the stable atmospheric boundary layer. *Boundary Layer Meteorology* **114**: 519–538.

DeBeer CM, Pomeroy J. 2010. Simulation of the snowmelt runoff contributing area in a small alpine basin. *Hydrology and Earth System Sciences Discussions* **7**: 971–1003.

Flerchinger GN, Cooley KR, Deng Y. 1994. Impacts of spatially and temporally varying snowmelt on subsurface flow in a mountainous watershed: 1. Snowmelt simulation. *Hydrological Sciences* **39**: 507–519.

Foken T, Wichura B. 1996. Tools for quality assessment of surface-based flux measurements. *Agricultural and Forest Meteorology* **78**: 83–105.

Garen D, Marks D. 2005. Spatially distributed energy balance snowmelt modelling in a mountainous river basin: estimation of meteorological inputs and verification of model results. *Journal of Hydrology* **315**: 126–153.

Green IRA, Stephenson D. 1986. Criteria for comparison of single event models. *Hydrological Sciences Journal* **31**: 395–411.

Hanson C. 2001. Long-term precipitation database, Reynolds Creek Experimental Watershed, Idaho, USA. *Water Resources Research* **37**: 2831–2834.

Harding R, Pomeroy J. 1996. The energy balance of the winter boreal landscape. *Journal of Climate* **9**: 2778–2787

van Heeswijk M, Kimball J, Marks D. 1996. Simulation of water available for runoff in clearcut forest openings during rain-on-snow events in the western Cascade Range of Oregon and Washington. In *USGS Water-Resources Investigations Report*. U.S. Geological Survey: Tacoma, Washington; 67.

Helgason W, Pomeroy J. 2012a. Characteristics of the near-surface boundary layer within a mountain valley during winter. *Journal of Applied Meteorology and Climatology* **51**: 583–597.

Helgason W, Pomeroy J. 2012b. Problems closing the energy balance over a homogeneous snow cover during midwinter. *Journal of Hydrometeorology* **13**: 557–572.

Johnson J, Marks D. 2004. The detection and correction of snow water equivalent pressure sensor errors. *Hydrological Processes* **18**: 3513–3525.

Jordan R. 1991. A one-dimensional temperature model for a snow cover: technical documentation for SNTHERM.89. In *CRREL Special Report*. U.S. Army Corps of Engineers Cold Regions Research and Engineering Laboratory: Hanover, New Hampshire; 49.

Kader BA, Yaglom AM. 1990. Mean fields and fluctuation moments in unstably stratified turbulent boundary layers. *Journal of Fluid Mechanics* **212**: 637–662.

Kaimal JC, Finnigan JJ. 1994. *Atmospheric Boundary Layer Flows – Their Structure and Measurement*. Oxford University Press: New York, NY; 289.

Lee Y-H, Mahrt L. 2004. An evaluation of snowmelt and sublimation over short vegetation in land surface modeling. *Hydrological Processes* **18**: 3543–3557.

Link T, Marks D. 1999a. Distributed simulation of snowcover mass- and energy balance in a boreal forest. *Hydrological Processes* **13**: 2439–2452.

Link T, Marks D. 1999b. Point simulation of seasonal snow cover dynamics beneath boreal forest canopies. *Journal of Geophysical Research* **104**: 27,841–827,857.

MacDonald MK, Pomeroy J, Pietroniro A. 2009. Parameterizing redistribution and sublimation of blowing snow for hydrological models: tests in a mountainous subarctic catchment. *Hydrological Processes* **23**: 2570–2583.

Mahrt L, Vickers D. 2005. Moisture fluxes over snow with and without protruding vegetation. *Quarterly Journal of the Royal Meteorological Society* **131**: 1251–1270.

Marks D, Dozier J. 1992. Climate and energy exchange at the snow surface in the alpine region of the Sierra Nevada: 2. Snow cover energy balance. *Water Resources Research* **28**: 3043–3054.

Marks D, Winstral A. 2001. Comparison of snow deposition, the snowcover energy balance, and snowmelt at two sites in a semi-arid mountain basin. *Journal of Hydrometeorology* **2**: 213–227.

Marks D, Kimball J, Tingey D, Link T. 1998. The sensitivity of snowmelt processes to climate conditions and forest cover during rain-on-snow: a study of the 1996 Pacific Northwest flood. *Hydrological Processes* **12**: 1569–1587.

Marks D, Domingo J, Susong D, Link TE, Garen D. 1999. A spatially distributed energy balance snowmelt model for application in mountain basins. *Hydrological Processes* **13**: 1935–1959.

Marks D, Cooley KR, Robertson DC, Winstral A. 2001a. Long-term snow database, Reynolds Creek Experimental Watershed, Idaho, USA. *Water Resources Research* **37**: 2835–2838.

Marks D, Link T, Winstral A, Garen D. 2001b. Simulating snowmelt processes during rain-on-snow over a semi-arid mountain basin. *Annals of Glaciology* **32**: 195–202.

Marks D, Winstral A, Seyfried M. 2002. Simulation of terrain and forest shelter effects on patterns of snow deposition, snowmelt and runoff over a semi-arid mountain catchment. *Hydrological Processes* **16**: 3605–3626.

Marks D, Reba ML, Pomeroy J, Link T, Winstral A, Flerchinger G, Elder K. 2008. Comparing simulated and measured sensible and latent heat fluxes over snow under a pine canopy. *Journal of Hydrometeorology* **9**: 1506–1522.

McCabe GJ, Clark MP. 2005. Trends and variability in snowmelt runoff in the western United States. *Journal of Hydrometeorology* **6**: 476–482.

Molotch NP, Blanken PD, Williams MW, Turnipseed A, Monson R, Margulis SA. 2007. Estimating sublimation of intercepted and sub-canopy snow using eddy covariance systems. *Hydrological Processes* **21**: 1567–1575.

Mote P, Hamlet A, Salathe E. 2008. Has spring snowpack declined in the Washington Cascades? *Hydrology and Earth System Sciences* **12**: 193–206.

Nakai Y, Sakamoto T, Terajima T, Kitamura K, Shirai T. 1999. Energy balance above a boreal coniferous forest: a difference in turbulent fluxes between snow-covered and snow-free canopies. *Hydrological Processes* **13**: 515–529.

Nash JE, Sutcliffe JV. 1970. River flow forecasting through concpetual models, part I – a discussion of principals. *Journal of Hydrology* **10**: 282–290.

Nayak A, Marks D, Chandler DG, Seyfried M. 2010. Long-term snow, climate, and streamflow trends at the Reynolds Creek Experimental Watershed, Owyhee Mountains, Idaho, United States. *Water Resources Research* **46**: W06519.

Nayak A, Marks D, Chandler D, Winstral A. 2012. Modeling inter-annual variability in snowcover development and melt at a semi-arid mountain catchment. *Journal of Hydrologic Engineering* **17**: 74–85.

Nolin A, Dozier J. 1993. Estimating snow grain size using AVIRIS data. *Remote Sensing of Environment* **44**: 1–8.

Paeschke W. 1937. Experimentelle Untersuchungen zum Rauhigkeits- and Stabilitätsproblem in der bodennahen Luftschicht. *Beiträge z. Phys. d. frein Atmos.* **24**: 163–189.

Paulson CA. 1970. The mathematical representation of wind speed and temperature profiles in the unstable atmospheric surface layer. *Journal of Applied Meteorology* **9**: 857–861.

Pomeroy JW, Gray DM. 1995. Snow accumulation, relocation and management. National Hydrology Research Institute Science Report No. 7. Environment Canada: Saskatoon. 144 pp.

Pomeroy J, Gray D, Shook K, Toth B, Essery R, Pietroniro A, Hedstrom N. 1998. An evaluation of snow accumulation and ablation processes for land surface modelling. *Hydrological Processes* **12**: 2339–2367.

Pomeroy J, Toth B, Granger R, Hedstrom N, Essery R. 2003. Variation in surface energetics during snowmelt in complex terrain. *Journal of Hydrometeorology* **4**: 702–716.

Reba ML, Link TE, Marks D, Pomeroy J. 2009. An assessment of corrections for eddy covariance measured turbulent fluxes over snow in mountain environments. *Water Resources Research* **45**: W00D38.

Reba ML, Marks D, Pomeroy J, Link T. 2011a. Estimating sublimation losses from snowpacks in a mountain catchment using eddy covariance and turbulent transfer. *Hydrological Processes*.

Reba ML, Marks D, Winstral A, Link TE, Kumar M. 2011b. Sensitivity of the snowcover energetics in a mountain basin to variations in climate. *Hydrologic Processes* **25**: 3312–3321.

Rebmann C, Gockede M, Foken T, Aubinet M, Aurela M, Berbigier P, Bernhofer C, Buchmann N, Carrara A, Cescatti A, Cuelemans R, Clement R, Elbers JA, Granier A, Grunwald T, Guyon D, Havrankova K, Heinesch B, Knohl A, Laurila T, Longdoz B, Marcolla B, Markkanen T, Miglietta F, Moncrieff J, Montagnani L, Moors E, Nardino M, Ourcival JM, Rambal S, Rannik U, Rotenberg E, Sedlak P, Unterhuber G, Vesala T, Yakir D. 2005. Quality analysis applied on eddy covariance measurements at complex forest sites using footprint modelling. *Theoretical and Applied Climatology* **89**: 121–141. DOI: 10.1007/s00704-004-0095-y.

Schmid HP. 1997. Experimental design for flux measurements: matching scale of observations and fluxes. *Agricultural and Forest Meteorology* **87**: 179–200.

Schotanus P, Nieuwstadt FTM, De Bruin HAR. 1983. Temperature measurement with sonic anemometer and its application to heat and moisture fluxes. *Boundary Layer Meteorology* **26**: 81–93.

Seyfried M, Grant L. 2007. Temperature effects on soil dielectric properties measured at 50 MHz. *Vadose Zone Journal* **6**: 759–765.

Seyfried M, Grant LE, Marks D, Winstral A, McNamara JP. 2009a. Simulated soil water storage effects on streamflow generation in a mountainous snowmelt environment, Idaho, USA. *Hydrologic Processes* **23**: 858–873.

Seyfried MS, Grant LE, Winstral A, Marks D, McNamara JP. 2009b. Simulated soil water storage effects on streamflow generation in a mountainous snowmelt environment, Idaho, USA. *Hydrologic Processes* **23**: 858–873.

Slaughter CW, Marks D, Flerchinger GN, VanVactor SS, Burgess M. 2001. Thirty-five years of research data collection at the Reynolds Creek Experimental Watershed, Idaho, United States. *Water Resources Research* **37**: 2819–2823.

Stewart I, Cayan D, Dettinger M. 2005. Changes towards earlier streamflow timing across Western North America. *Journal of Climate* **18**: 1136–1155.

Tarboton DG, Luce CH. 1996. Utah Energy Balance Snow Accumulation and Melt Model (UEB). Computer model technical description and users guide. In *USDA Forest Service Report*. Utah Water Research Laboratory and USDA Forest Service Intermountain Research Station.; 63.

Turnipseed AA, Anderson DE, Blanken PD, Baugh WM, Monson RK. 2003. Airflows and turbulent flux measurements in mountainous terrain. Part 1. Canopy and local effects. *Agricultural and Forest Meteorology* **119**: 1–21.

Twine TE, Kustas W, Norman JM, Cook DR, Houser PR, Meyers TP, Prueger JH, Starks PJ, Wesely ML. 2000. Correcting eddy–covariance flux underestimates over a grassland. . *Agricultural and Forest Meteorology* **103**: 279–300.

Vickers D, Mahrt L. 1997. Quality control and flux sampling problems for tower and aircraft data. *Journal of Atmospheric and Ocean Technology* **14**: 512–526.

Vickers D, Mahrt L. 2003. The cospectral gap and turbulent flux calculations. *Journal of Atmospheric and Ocean Technology* **20**: 660–672.

Webb EK. 1970. Profile relationships: the log-linear range, and extension to strong stability. *Quarterly Journal of the Royal Meteorological Society* **96**: 67–90.

Webb EK, Pearman GI, Leuning R. 1980. Correction of flux measurements for density effects due to heat and water vapor transfer. *Quarterly Journal of the Royal Meteorological Society* **106**: 85-100.

Wilson K, Goldstein A, Falge E, Aubinet M, Baldocchi D, Berbigier P, Bernhofer C, Reinhart C, Dolman H, Field C, Grelle A, Ibrom A, Law BE, Kowalski A, Meyers T, Moncrieff J, Monson R, Oechel WC, Tenhunen J, Valentini R, Verma SB. 2002. Energy balance closure at FLUXNET sites. *Agricultural and Forest Meteorology* **113**: 223–243.

Winstral A, Marks D. 2002. Simulating wind fields and snow redistribution using terrain-based parameters to model snow accumulation and melt over a semi-arid mountain catchment. *Hydrological Processes* **16**: 3585–3603.

Winstral A, Marks D, Gurney RJ. 2009. An efficient method for distributing wind speeds over heterogeneous terrain. *Hydrological Processes* **23**: 2526–2535.

Yasuda N. 1988. Turbulent diffusivity and diurnal variations in the atmospheric boundary layer. *Boundary Layer Meteorology* **43**: 209–221.